p-ISSN 2615-787X e-ISSN 2615-790X
Accredited by Directorate General of Higher Education, Research, and Technology, Republic of Indonesia, No. 225/E/KPT/2022

Tropical Animal Science Journal, January 2026, 49(1):19-29
DOI: https://doi.org/10.5398/tasj.2026.49.1.19
Available online at https://journal.ipb.ac.id/index.php/tasj

Integrated Metabolomic and Functional Assessment of Sexed Frozen Semen in Holstein Friesian Bulls

M. Yusuf[a,*], A. M. Diansyah[a], S. Sahiruddin[a], M. Masturi[a], T. Maulana[b], S. Said[b], R. Rahmat[c], A. M. Alfian[a], A. A. S. Adam[a], A. N. H. S. Yusri[a], A. Nurlatifah[d], & M. F. Amrullah[e]

[a] Department of Animal Production, Faculty of Animal Science, Hasanuddin University, Jl. Perintis Kemerdekaan Km.10, Makassar 90245, Indonesia
[b] Research Center for Applied Zoology, National Research and Innovation Agency, Cibinong 16911, Indonesia
[c] Department of Animal Science, Faculty of Agriculture, Lambung Mangkurat University, Jl. A. Yani Km 36, Banjarmasin 70714, Indonesia
[d] Department of Nutrition and Feed Science, Faculty of Animal Science, Gadjah Mada University, Yogyakarta 55281, Indonesia
[e] Doctoral Program of Animal Biomedical Science, School of Veterinary Medicine and Biomedical Science, IPB University, Jl. Agatis, Kampus IPB Darmaga Bogor 16680, Indonesia
*Corresponding author: myusuf@unhas.ac.id
(Received 22-08-2025; Revised 29-10-2025; Accepted 31-10-2025)

ABSTRACT

This study examined the differences in sperm quality and metabolite profiles among X and Y sperm in Holstein Friesian bulls. It also tried to find specific metabolites that can help improve the accuracy of sexed semen use in humid tropical dairy farms. Semen samples from five bulls were separated by sex and tested for movement, live sperm count, shape, and membrane and acrosome health. The tests used Computer-Assisted Sperm Analysis (CASA) and regular microscope checks. Metabolite analysis was performed using LC-HRMS, followed by various statistical tests, pathway checks, and ROC curve analysis. The outcomes showed that X sperm had better movement and acrosome health, while Y sperm had stronger membranes, fewer shape problems, and moved faster. The untargeted metabolite study showed clear differences between the two groups. X sperm had more identified metabolites and greater average levels. The crucial metabolites found more in X sperm were D-(−)-fructose, L-(+)-lactic acid, and sn-glycero-3-phosphocholine. Meanwhile, Y sperm had greater levels of acetyl-L-carnitine. The pathway analysis showed that X sperm primarily utilized carbohydrate and fat processing through glycolysis and phosphocholine pathways to maintain their movement and membrane integrity. On the other hand, Y sperm mainly use a carnitine-based energy pathway to support their faster and straighter movement. The identified metabolites can serve as reliable biomarkers to aid in laboratory quality control checks and enhance the quality of semen extenders. This outcome gives a good way to make sexed semen more stable and reliable in tropical dairy farming conditions.

Keywords: biomarkers; Holstein Friesian bulls; metabolomic profiling; sex-sorted spermatozoa; sperm quality

INTRODUCTION

Sex sorting of bull semen is now commonly used in dairy farming to produce more female calves, speed up genetic improvement, and make herd replacement easier to plan. However, the quality of sex-sorted semen is often different among bulls and herds. The pregnancy rates are usually lower than when utilizing regular semen (Thongkham *et al*., 2021; Álvarez Gallardo *et al*., 2024). This difference makes it harder for farmers to make good decisions. It also reveals the need for biological markers to predict how well the semen will work, not just describe its traits.

Sperm function depends mainly on energy supply, membrane structure, and redox balance. There is a careful balance between making ATP and producing reactive oxygen, revealing a trade-off between energy use and stress. ATP comes from two sources: mitochondrial energy in the midpiece and glycolysis in the tail (Amaral, 2022; Ricci *et al*., 2023; Schmidt *et al*., 2024). These factors affect how the tail moves, which controls sperm movement. These energy limits also affect how ready the sperm is for capacitation, how long it can keep moving, and how well it survives during processing and storage.

Metabolomics helps us understand these biological processes as a whole system. Earlier studies drew a clear link between metabolite patterns and fertility in bulls, in both fresh and frozen semen. They found certain metabolites and pathways that can separate

high fertility bulls from low fertility (Talluri *et al*., 2022; Giaretta *et al*., 2025). These outcomes reveal that studying small molecules can give useful biochemical markers to support regular sperm quality tests.

The environment strongly affects semen quality and molecular signals. Heat stress is known to lower semen quality in bulls, and its effects can last for weeks after being exposed to high temperatures. Changes in fertility by season also reveal that heat stress may have delayed effects on sperm production (Capeta *et al*., 2022; Khan *et al*., 2023). These environmental problems are very crucial in humid tropical areas like Indonesia. Constant heat, uneven energy in forage diets, and weak cold storage systems can disturb the balance between glycolytic and oxidative energy use. They can also change membrane lipids and affect the success of sex sorting (Silva *et al*., 2023). Even though global interest in this topic is increasing, there is still little research on how metabolite patterns differ among X and Y sperm and how these differences relate to semen quality and movement. This lack of knowledge is obvious in tropical dairy farms in Indonesia (Chang *et al*., 2025).

Even though more people worldwide are interested in this topic, there is still little research on the differences in metabolite patterns among X and Y sperm and how these differences relate to semen quality and movement. This lack of information is especially clear in tropical dairy farms in Indonesia (Chang *et al*., 2025). Firdaus *et al*. (2024) found a pregnancy rate of about 63% utilizing albumin-sedimented sexed semen, which was greater than unsexed or PDGC-sexed semen (around 47%). Nurcholis *et al*. (2025) also found pregnancy rates of 65% and 86%, depending on the season and semen type. Overall, these outcomes reveal that sex-sorted semen can give similar fertility outcomes to regular semen, but its performance in the field is still not stable in Indonesia.

This study looks for metabolite markers that clearly show the difference between X and Y sperm in sex-sorted Holstein Friesian bulls. It also studies how these metabolites relate to semen quality and sperm movement. Ultimately, this research aims to find useful markers that can be used in Indonesia's humid tropical dairy farms.

MATERIALS AND METHODS

Experimental Design and Ethical Approval

This study was done at the Animal Reproduction Laboratory, Semen Processing Unit, Faculty of Animal Husbandry, Hasanuddin University, Makassar, Indonesia. The metabolite analysis was done at the Center for Applied Zoology Research, BRIN, Cibinong, Indonesia. Sex-sorted semen samples came from five Holstein Friesian bulls by five different batch codes from the Artificial Insemination Center (AIC) in Lembang, West Java, Indonesia. The semen was separated by sex utilizing an albumin column method. After that, the samples were frozen in 0.25 mL straws with a Tris–egg yolk (TEY) extender and glycerol, following standard procedures used in Indonesian AI centers (Santoso *et al*., 2021; Baharun *et al*., 2025). Reports by the field reveal that sexed semen can produce the desired calf sex by 80%–85% accuracy, and the pregnancy rates are similar to regular semen (Said *et al*., 2014). This study was approved by the Animal Use Ethics Committee for Research and Education, Faculty of Animal Science, Hasanuddin University (Approval No. 015/UN4.12/EC/VI/2025).

Sperm Evaluation

Sperm movement was checked by putting 10 μL of semen on a glass slide and analyzing it using a Computer-Assisted Sperm Analysis (CASA) system utilizing Vision Version 3.7.5 software (Minitube, Germany). The system was connected to a Primo Star microscope (Zeiss, Germany) at 200× magnification, following Diansyah *et al*. (2024). Sperm shape problems and live sperm count were checked using the Nirmala *et al.* method (2025). Ten μL of semen was mixed with ten μL of 2% eosin on a glass slide. After the smear dried, it was checked under a Primo Star trinocular microscope (Zeiss, Germany) at 400× magnification by Indomicro View 3.7 software. Sperm that turned red were counted as dead, and sperm that stayed clear were counted as alive. At least 200 sperm were checked in each sample to get reliable outcomes. Sperm with bent or broken tails or odd-shaped heads were counted as abnormal. Some tail damage can happen during slide preparation because of handling, not because the sperm were actually abnormal. Acrosome health was checked using the Fadilla *et al*. method (2023). Semen samples were mixed with a formalin–saline solution (NaCl with 1% formalin) in a 1:4 ratio. The samples were then examined under a microscope (Zeiss, Germany) to see the acrosome condition. Sperm with healthy acrosomes were seen as having dark-stained heads. Membrane health was checked utilizing the hypoosmotic swelling test (HOST). Ten μL of semen was mixed with HOST solution (0.179 g NaCl in 100 mL of water) and kept at 37 °C for 30 minutes. Then the samples were observed under a Primo Star trinocular microscope (Zeiss, Germany). Sperm with curved tails were counted as having healthy membranes, and those with straight tails were counted as damaged.

Metabolomic Analysis

Metabolomic profiling was conducted utilizing an LC–HRMS platform following the procedure described by Longobardi *et al.* (2020). Samples stored at −20 °C were thawed at 4 °C prior to analysis. An aliquot of 100 μL from each sample was mixed with 400 μL of cold methanol/acetonitrile (1:1, v/v), thoroughly vortexed, and centrifuged at 14,000 × g for 20 minutes at 4 °C to precipitate proteins. The resulting supernatant was transferred to new tubes and dried utilizing a vacuum centrifuge. The dried residues were reconstituted in 100 μL of acetonitrile/water (1:1, v/v), centrifuged again at 14,000 × g for 15 minutes at 4 °C, filtered through 0.2 μm membranes, and finally transferred into LC glass vials for analysis. Liquid chromatography was performed

utilizing a Horizon UHPLC system (Thermo Scientific™ Vanquish™, Germany) equipped with a binary pump (Germering, Germany) and a Hypersil GOLD column (150 mm × 2.1 mm i.d., 1.9 μm; Thermo Scientific™ Hypersil GOLD™, Lithuania). The mobile phases consisted of (A) LC–MS grade water containing 0.1% formic acid and (B) LC–MS grade acetonitrile containing 0.1% formic acid (Fisher Chemical, Optima LC–MS Grade). Chromatographic separation was performed at a flow rate of 0.2 mL min^{-1} utilizing a 24-minute gradient program as follows: 0–1.5 min, 2% B; 1.5–4.5 min, 2%–12% B; 4.5–7 min, 12% B; 7–12 min, 12%–24% B; 12–15 min, 24%–48% B; 15–16 min, 48%–60% B; 16–17 min, 60%–100% B; 17–19 min, 100% B (isocratic); 19–20 min, 100–2% B; and 20–24 min, 2% B for column re-equilibration. The column temperature was maintained at 35 °C, and the injection volume was set to 5 μL. High-resolution mass spectrometry was conducted utilizing an Orbitrap Exploris 240 Mass Spectrometer (Thermo Scientific™ Orbitrap™ Exploris 240, Bremen, Germany) operating in Full MS/dd-MS^2 mode by polarity switching among positive and negative ionization. The Full MS parameters were set as follows: resolution 60,000 (FWHM), scan range m/z 70–1000, maximum injection time 100 ms, intensity threshold 5,000, singly charged precursors, and a mass tolerance of ±5 ppm. Data-dependent MS^2 acquisition was performed at a resolution of 22,500 (FWHM) utilizing stepped normalized collision energies of 30, 50, and 80, by nitrogen as the collision gas. Ionization was carried out utilizing an OptaMax™ NG heated electrospray ionization (H-ESI) source, by spray voltages of +3,500 V (positive mode) and −2,500 V (negative mode). The sheath gas, auxiliary gas, and sweep gas were set to 30, 7, and 1 arbitrary units (AU), respectively. The ion transfer tube temperature was maintained at 275 °C, and the vaporizer temperature at 320 °C. Data processing was performed utilizing Thermo Scientific Compound Discoverer 3.3 software (San Jose, USA). MS/MS spectral matching was performed utilizing the mzCloud (All) library. Mass-list searches and feature annotations were conducted by reference to several databases, including the Endogenous Metabolites database (~4,400 compounds), LIPID MAPS Structure Database (version 2023-01-11), Natural Products Atlas 2021_08 EFS HRAM Compound Database, Extractables and Leachables HRAM Compound Database (2023 update), and FCCDB_2022. ChemSpider integration was employed to enhance metabolite annotation through multiple databases, including the Bovine Metabolome Database, Bovine Rumen Metabolome Database, ChEBI, ChEMBL, KEGG, LIPID MAPS, MDPI, Natural Product Updates, Nature Chemical Biology, Nature Chemistry, Nature Communications, NIST Spectra, Peptides, PubChem, ScienceBase, and Springer Nature.

Statistical Analysis and Bioinformatics

Semen quality parameters and sperm motility characteristics were analyzed utilizing SPSS version 20.0 (IBM Corp., Armonk, NY, USA). Data normality was assessed utilizing the Shapiro–Wilk test, and homogeneity of variances was evaluated utilizing Levene's test. Comparisons among X- and Y-chromosome–bearing spermatozoa were performed utilizing independent-samples t-tests, and outcomes were presented as mean ± standard deviation (SD). All statistical analyses were two-sided, with a significance threshold set at $\alpha = 0.05$. For metabolite analysis, the peak intensity data by Compound Discoverer 3.3 were processed by MetaboAnalyst 6.0 (www.metaboanalyst.ca). Before the analysis, the intensity values were changed utilizing $\log_2(x + 1)$ and then auto-scaled. Variables with too many missing values were removed. The remaining missing values were filled by a small number equal to half of the lowest detected value. Principal component analysis (PCA) was first used as an unsupervised method to see general patterns and differences in the data. Next, partial least squares–discriminant analysis (PLS-DA) was used to separate the sample groups. The model's reliability was checked by k-fold cross-validation and permutation tests utilizing the default settings in MetaboAnalyst. Crucial variables that helped separate the groups were then selected for further study.

For single-variable analysis, two-tailed t-tests were used to check the differences in metabolite levels among groups. If needed, p-values were corrected utilizing the Benjamini–Hochberg FDR method. Heatmaps by hierarchical clustering were made by $\log_{10}$-transformed data utilizing Euclidean distance and Ward's linkage method. Pathway enrichment and topology were analyzed utilizing KEGG and HMDB reference sets. Enrichment was checked by a hypergeometric test, and pathway structure was measured by relative amongness centrality. Pathways with FDR-adjusted p-values below 0.05 were counted as significant. Finally, the potential of metabolites as biomarkers was tested utilizing ROC curve analysis by Monte Carlo cross-validation (balanced subsampling). The area under the curve (AUC) was used as the main performance measure.

RESULTS

Sperm Quality and Kinematics

Semen quality and movement were different among X and Y sperm (Table 1). X sperm had better movement and acrosome health, while Y sperm had stronger membranes and fewer shape problems. There was no significant difference in live sperm among the two groups. For CASA outcomes, Y sperm drawn greater VCL, VAP, and VSL (speed measures), bigger head movement (DCL, DAP, DSL), and greater straightness (STR). Linearity (LIN) was the same for both groups, but wobble (WOB) was greater in X sperm. Overall, Y sperm moved faster and more efficiently, while X sperm had better overall movement and acrosome health.

Metabolomic Data
Study Samples and Data Overview

Untargeted LC–HRMS analysis found similar metabolite peaks in both X and Y sperm (Table 2). After quality control and HMDB-based labeling, more

features were kept for X sperm, and their average peak intensity was also greater than that of Y sperm.

Principal Component Analysis (PCA) and Partial Least Squares Discriminant Analysis (PLS-DA)

Principal component analysis (PCA) of the LC–HRMS data showed a clear difference between X and Y sperm (Figure 1). The first and second principal components (PC1 and PC2) explained 51.0% and 37.2% of the variation. The PC1–PC2 scores drawn two clear, separate clusters with slight variation inside each group, as revealed by the 95% confidence ellipses (Figure 1B).

Table 1. Sperm quality and kinematic variables of X- and Y-bearing spermatozoa of Holstein Friesian bulls

Variables	Sexed sperm (Mean ± SD)	
	X-Sperm	Y-Sperm
Motility (%)	58.04 ± 1.62[a]	53.66 ± 1.78[b]
Viability (%)	8.48 ± 1.06[a]	9.72 ± 1.23[a]
Abnormality (%)	72.27 ± 2.12[a]	68.04 ± 1.37[b]
Membrane integrity (%)	66.92 ± 0.88[a]	83.05 ± 2.17[b]
Acrosome integrity (%)	69.79 ± 0.66[a]	63.93 ± 0.98[b]
VCL (μm/s)	124.37 ± 2.97[a]	147.16 ± 3.12[b]
VAP (μm/s)	115.58 ± 4.23[a]	121.96 ± 2.3[b]
VSL (μm/s)	104.96 ± 2.56[a]	114.82 ± 2.68[b]
DCL (μm)	96.15 ± 3.55[a]	219.17 ± 4.19[b]
DAP (μm)	84.47 ± 1.95[a]	165.92 ± 3.34[b]
DSL (μm)	78.47 ± 1.35[a]	160.94 ± 4.53[b]
LIN (%)	71.77 ± 1.76[a]	73.6 ± 3.24[a]
STR (%)	82.17 ± 1.12[a]	92.98 ± 1.97[b]
WOB (%)	87.62 ± 2.01[a]	78.91 ± 3.07[b]

Note: Values by different superscript letters (a-b) in the same row indicate a statistically significant difference among X- and Y-bearing spermatozoa (p<0.05). VCL = curvilinear velocity; VAP = average path velocity; VSL = straight-line velocity; DCL = curvilinear distance; DAP = average path distance; DSL = straight-line distance; LIN = linearity; STR = straightness; WOB = wobble.

Pairwise score–density plots (Figure 1A) also showed clear differences among X and Y sperm in several principal components (p<0.05), giving strong proof of fundamental metabolite differences among the two groups.

Supervised PLS-DA of the metabolite data showed a clear separation between X and Y sperm on the first two components (Figure 2). Components 1 and 2 explained 50.0% and 35.4% of the variation. The 95% confidence ellipses for the two groups did not overlap, revealing a clear difference between them.

Differential Metabolomic Profiles

A total of 25 metabolites were different between X and Y sperm (Figure 3; Table 3). More metabolites had greater peak intensities in X sperm than in Y sperm. Some metabolites were almost unique to one group by significant fold changes, while others showed more minor changes, making a clear two-way pattern in the volcano plot. The hierarchical heatmap grouped samples by their chromosome type and groups of metabolites showing consistent increases or decreases in metabolite peak areas within each group (Figure 4). These outcomes suggest that the differences seen are broad metabolic changes, not just changes in single metabolites. Besides these trends, the top ten crucial features ranked by VIP made a small, clear group (Figure 5) that followed the two-way pattern: about half

Table 2. Characteristics of sex-sorted semen samples (X- and Y-bearing spermatozoa) and overview of metabolomic data obtained by Holstein Friesian bulls

Variables	X Sperm	Y Sperm
Detected metabolite peaks	194	195
Metabolites retained after QC (HMDB)	111	94
Avg. peak area (×10⁶)	2.324.766	1.570.174

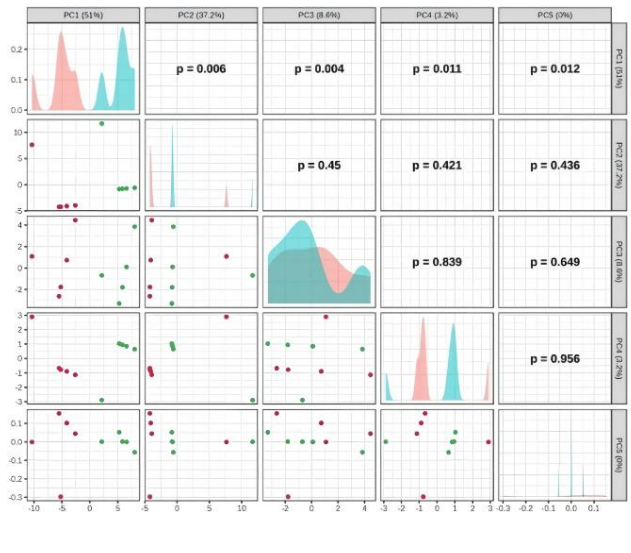

(A)

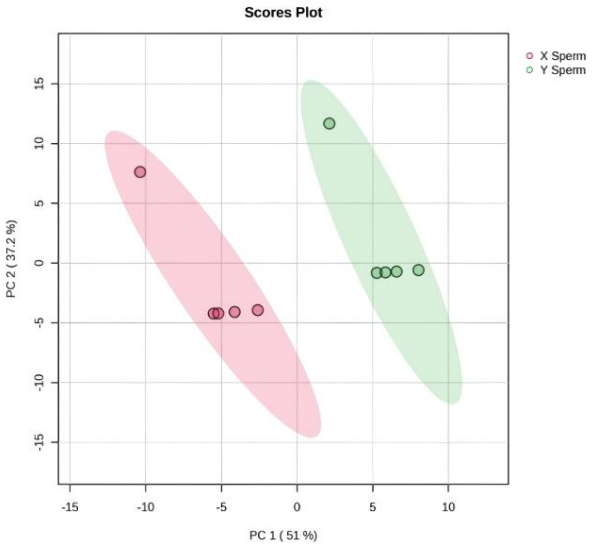

(B)

Figure 1. Principal component analysis (PCA) of metabolomic profiles by sex-sorted spermatozoa of Holstein Friesian bulls. (A) Pairwise scatter–density plots of principal component (PC) scores (PC1–PC5). (B) PCA scores plot (PC1 vs. PC2) revealing clear separation among X- and Y-bearing spermatozoa, by 95% confidence ellipses.

had greater peak areas in X sperm and the other half in Y sperm. This small group of metabolites seems to be the main reason for the clear separation between the two groups.

Pathway enrichment analysis showed that carbohydrate metabolism and membrane lipid changes were the main differences among X and Y sperm (Figure 6; Table 4). Crucial carbohydrate pathways—such as starch and sucrose, fructose and mannose, galactose, and amino sugar and nucleotide sugar metabolism—were the most significant, along with glycolysis/gluconeogenesis and pyruvate metabolism. Lipid pathways, such as glycerophospholipid and ether-lipid metabolism, were also found. Glycerophospholipid and fructose/mannose metabolism showed the most significant pathway impact, while lysine breakdown had a smaller effect. Overall, these outcomes match the energy and membrane differences between X and Y sperm.

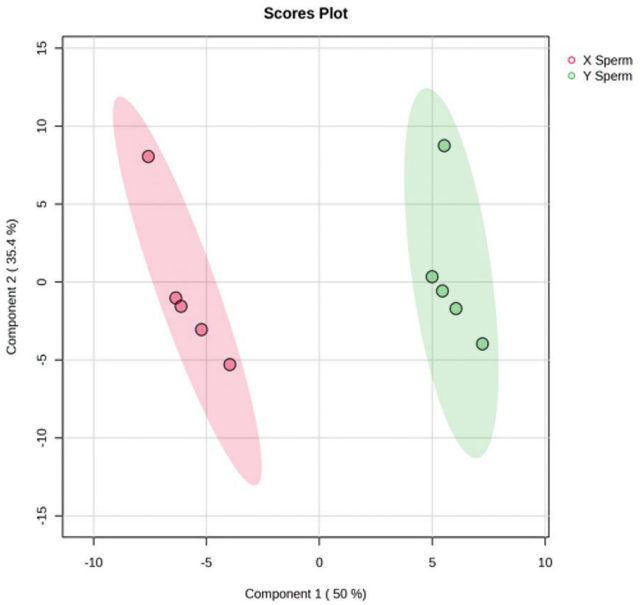

Figure 2. Partial least squares–discriminant analysis (PLS-DA) of LC–HRMS–derived metabolomic profiles by X- and Y-bearing spermatozoa of Holstein Friesian bulls, revealing clear separation among groups along the first two latent components, by 95% confidence ellipses.

Biomarker Performance (ROC Analysis)

Although ten features achieved perfect discrimination in the ROC analysis (Table 5), six of them exhibited truncated effect sizes ($|\log_2 FC| \approx 99$), reflecting metabolites detected in only one group (presence/absence after imputation). Because such quasi-separation can artificially inflate AUC values and is unlikely to generalize, these features were not considered primary biomarker candidates in the main analysis. We therefore prioritized four metabolites by physiologically meaningful fold-changes and consistent peak areas across samples: D-(−)-fructose, sn-glycerol-3-phosphocholine, and L-(+)-lactic acid (enriched in X-sperm), and acetyl-L-carnitine (enriched in Y-sperm). These four metabolites achieved an AUC of 1.00 in this dataset, as illustrated by their non-overlapping distributions in Figures 7A–D.

Correlations among Metabolites, Sperm Quality, and Kinematics

In X-bearing spermatozoa (Figure 8A), the three profiled metabolites—D-(−)-fructose, sn-glycerol-3-phosphocholine (sn-GPC), and L-(+)-lactic acid—showed generally positive correlations with key quality traits, including motility, viability, and membrane and acrosome integrity; meanwhile, sperm abnormalities were negatively correlated ($r \approx -0.42$ to -0.15). L-(+)-lactic acid showed the strongest

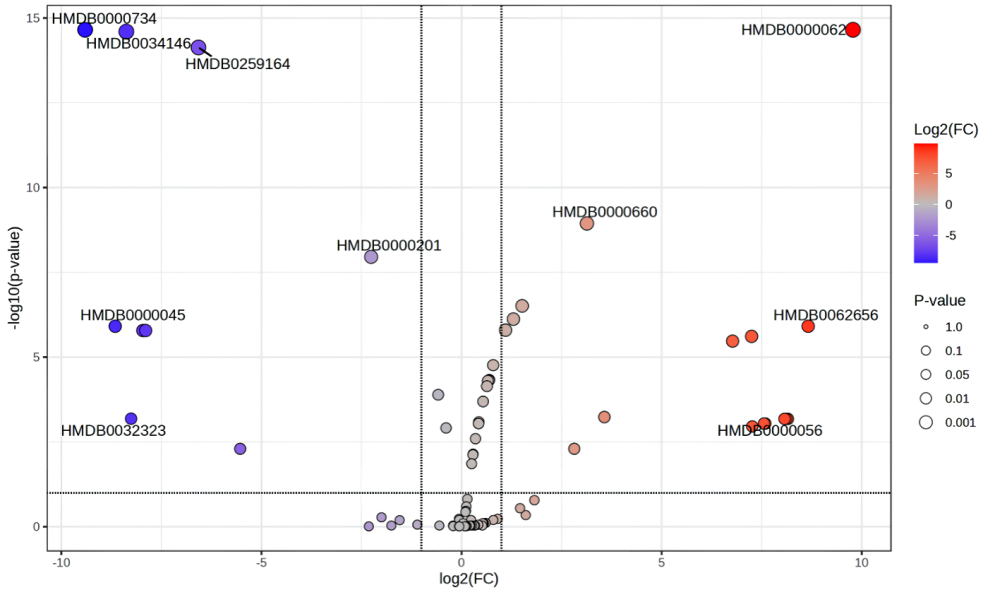

Figure 3. Volcano plot summarizing differential metabolite abundances among X- and Y-bearing spermatozoa of Holstein Friesian bulls. Red and blue points indicate greater metabolites in X- and Y-sperm, respectively ($p<0.05$).

Table 3. Differential metabolites identified among X- and Y-bearing spermatozoa of Holstein Friesian bulls based on LC–HRMS analysis

HMDB ID	m/z	RT (min)	log_2FC	FDR	Direction
HMDB0000062	162.1122	1.854	97.797	2.22×10^{-11}	X Sperm
HMDB0000734	188.07045	7.39	-94.055	2.22×10^{-11}	Y Sperm
HMDB0034146	284.29446	19.098	-83.758	2.53×10^{-11}	Y Sperm
HMDB0259164	267.17194	19.855	-65.738	7.37×10^{-11}	Y Sperm
HMDB0000660	179.056	1.838	31.327	1.14×10^{-5}	X Sperm
HMDB0000201	204.12272	2.297	-22.599	1.10×10^{-4}	Y Sperm
HMDB0000086	258.10971	1.803	15.139	3.08×10^{-3}	X Sperm
HMDB0000190	89.02433	2.224	12.958	7.55×10^{-3}	X Sperm
HMDB0062656	280.26324	20.395	86.612	1.23×10^{-2}	X Sperm
HMDB0000045	348.06982	2.099	-86.541	1.23×10^{-2}	Y Sperm
HMDB0034301	86.09628	2.23	10.995	1.60×10^{-2}	X Sperm
HMDB0000191	132.03024	1.745	-79.635	1.64×10^{-6}	Y Sperm
HMDB0303161	89.05959	15.76	-78.932	1.64×10^{-6}	Y Sperm
HMDB0032865	220.11189	19.501	72.477	2.44×10^{-2}	X Sperm
HMDB0014859	237.15926	7.571	67.717	3.37×10^{-2}	X Sperm
HMDB0000243	87.00867	2.176	35.685	5.84×10^{-4}	X Sperm
HMDB0032323	102.1276	21.577	-8.257	6.52×10^{-4}	Y Sperm
HMDB0000056	88.04033	6.34	81.545	6.61×10^{-4}	X Sperm
HMDB0000784	187.09747	15.47	81.125	6.61×10^{-4}	X Sperm
HMDB0002428	165.01915	8.84	80.698	6.61×10^{-4}	X Sperm
HMDB0003312	253.05049	16.33	75.913	9.08×10^{-4}	X Sperm
HMDB0037851	349.00186	15.768	75.562	9.08×10^{-4}	X Sperm
HMDB0033843	144.10184	2.01	72.642	1.10×10^{-3}	X Sperm
HMDB0040219	241.17796	19.221	-55.313	5.04×10^{-3}	Y Sperm
HMDB0000958	173.00906	2.18	28.162	5.04×10^{-3}	X Sperm
HMDB0034301	86.09628	2.23	10.995	2.22×10^{-11}	X Sperm

Note: log_2FC is calculated as X/Y; positive values = greater in X. RT = retention time; FDR = false discovery rate; HMDB = Human Metabolome Database.

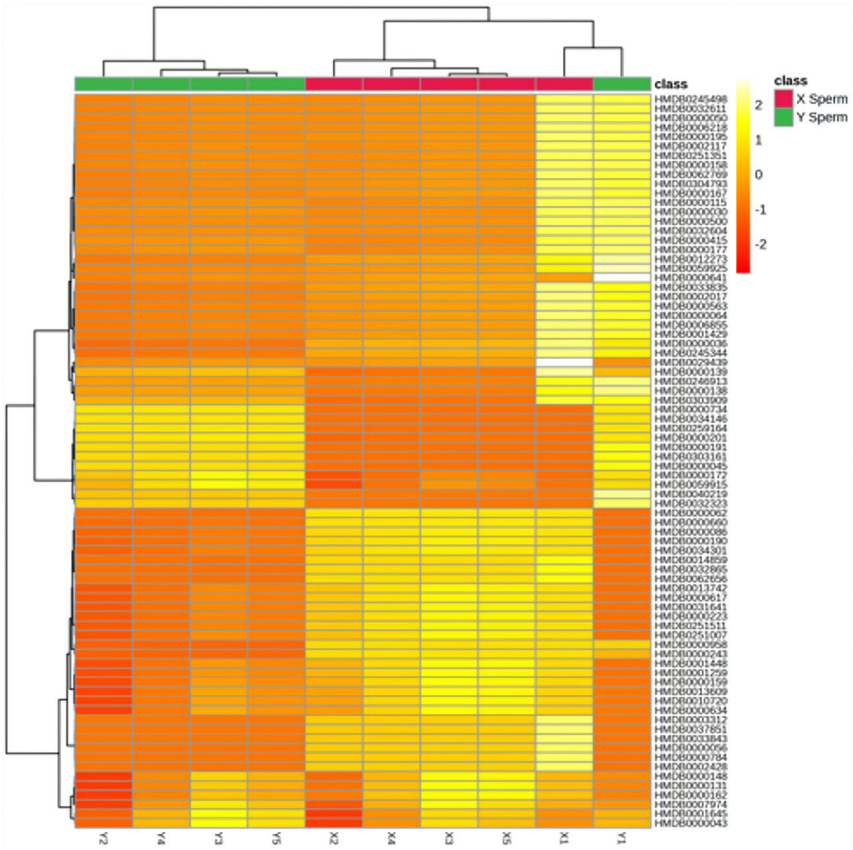

Figure 4. Hierarchical clustering heatmap of annotated metabolites in X- and Y-bearing spermatozoa of Holstein Friesian bulls. Columns represent individual samples, and rows represent metabolites. Dendrograms reveal clustering of samples primarily according to chromosomal type (X vs. Y).

correlations by membrane integrity (r ≈ 0.81) and track straightness (STR; r ≈ 0.86). Strong associations were also observed among kinematic parameters and the sugar/phosphocholine axis: wobble (WOB) correlated very strongly with D-(−)-fructose (r ≈ 0.98) and sn-glycerol-3-phosphocholine (sn-GPC; r ≈ 0.99), by additional positive correlations across linearity and velocity metrics (e.g., VSL, LIN, STR; r ≈ 0.78–0.86). In Y-bearing spermatozoa (Figure 8B), acetyl-L-carnitine displayed a selective association, correlating most strongly by progressive motility parameters—VSL (r =

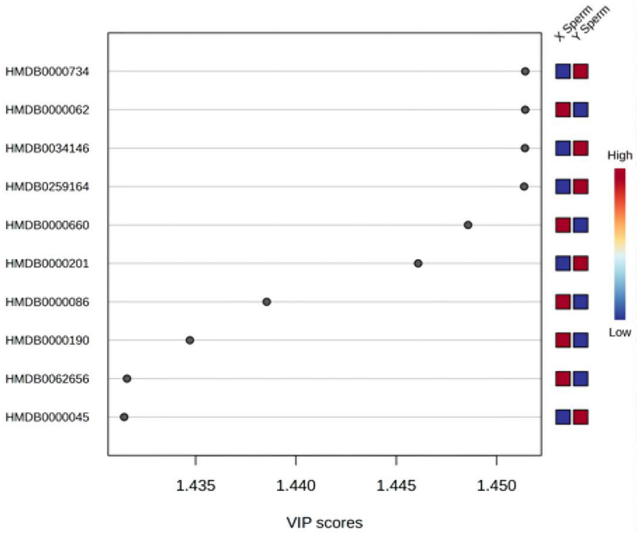

Figure 5. Variable Importance in Projection (VIP) plot displaying the top ten discriminant metabolites identified by the PLS-DA model in X- and Y-bearing spermatozoa of Holstein Friesian bulls. Color blocks indicate the group in which each metabolite exhibits greater peak intensity.

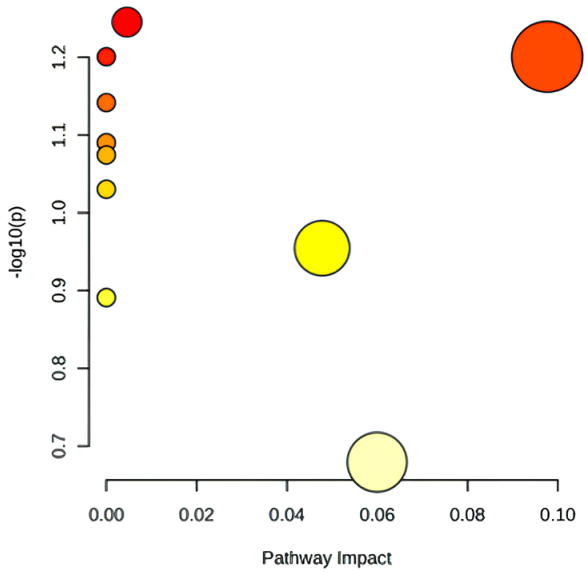

Figure 6. Bubble plot of pathway enrichment analysis showing significantly enriched KEGG/HMDB metabolic pathways that differentiate X- and Y-bearing spermatozoa of Holstein Friesian bulls. Each colored bubble represents one enriched metabolic pathway, with bubble size indicating pathway impact and bubble color intensity corresponding to $-\log_{10}$(p-value).

Table 4. Summary of enriched metabolic pathways differentiating X- and Y-bearing spermatozoa of Holstein Friesian bulls

Pathway name	HMDB ID	Match status	Raw p	Log_{10}(p)	Impact
Starch and sucrose metabolism	HMDB0000062	1/18	5.68×10^{-2}	12.454	4.57×10^{-3}
Ether lipid metabolism	HMDB0000734	1/20	6.30×10^{-2}	12.007	0
Fructose and mannose metabolism	HMDB0034146	1/20	6.30×10^{-2}	12.007	9.77×10^{-2}
Pyruvate metabolism	HMDB0259164	1/23	7.22×10^{-2}	11.417	0
Glycolysis or Gluconeogenesis	HMDB0000660	1/26	8.16×10^{-2}	10.901	0
Galactose metabolism	HMDB0000201	1/27	8.43×10^{-2}	10.743	0
Lysine degradation	HMDB0000086	1/30	9.33×10^{-2}	10.302	0
Glycerophospholipid metabolism	HMDB0000190	1/36	1.11×10^{-1}	0.95443	3.32×10^{-1}
Amino sugar and nucleotide sugar metabolism	HMDB0062656	1/42	1.29×10^{-1}	0.89085	0
Purine metabolism	HMDB0000045	1/71	2.09×10^{-1}	0.67911	6.00×10^{-2}

Note: Pathways were identified utilizing KEGG/HMDB references. Definitions: HMDB = human metabolome database; Raw p = unadjusted probability value; Impact = pathway topology score.

Table 5. Cross-validated ROC performance of the top ten candidate metabolite biomarkers distinguishing X- by Y-bearing spermatozoa of Holstein Friesian bulls

Metabolite	HMDB ID	AUC	p-Value	Log_2FC
trans-3-Indoleacrylic acid	HMDB0000734	1	5.01×10^{-17}	-99.00
DL-Carnitine	HMDB0000062	1	5.70×10^{-17}	99.00
Stearamide	HMDB0034146	1	9.71×10^{-17}	-99.00
Tributyl phosphate	HMDB0259164	1	3.78×10^{-16}	-99.00
D-(-)-Fructose	HMDB0000660	1	7.40×10^{-11}	3.1327
Acetyl-L-carnitine	HMDB0000201	1	8.49×10^{-10}	-2.5990
sn-glycero-3-Phosphocholine	HMDB0000086	1	2.76×10^{-8}	1.5139
L-(+)-Lactic acid	HMDB0000190	1	7.75×10^{-8}	1.2986
Linoleamide	HMDB0062656	1	$1.53E \times 10^{-7}$	99.00
Adenosine 5'-monophosphate	HMDB0000045	1	1.58×10^{-7}	-99.00

Note: AUC = area under the ROC curve; Log_2FC = $\log_2$ fold change; HMDB = Human Metabolome Database.

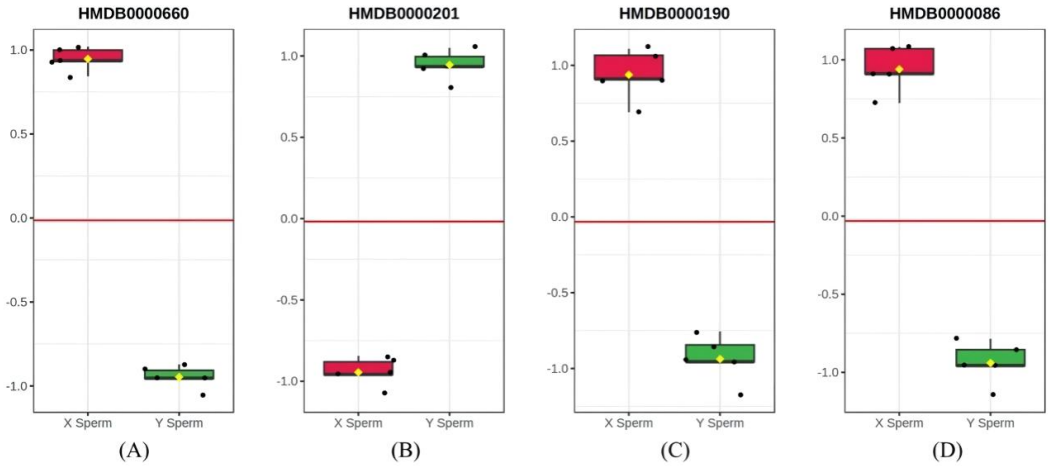

Figure 7. Boxplots depicting the relative abundances of the four top discriminatory metabolites—(A) D-(-)-fructose, (B) acetyl-L-carnitine, (C) sn-glycerol-3-phosphocholine, and (D) L-(+)-lactic acid—in X- and Y-bearing spermatozoa of Holstein Friesian bulls. Boxes represent the median and interquartile range (IQR).

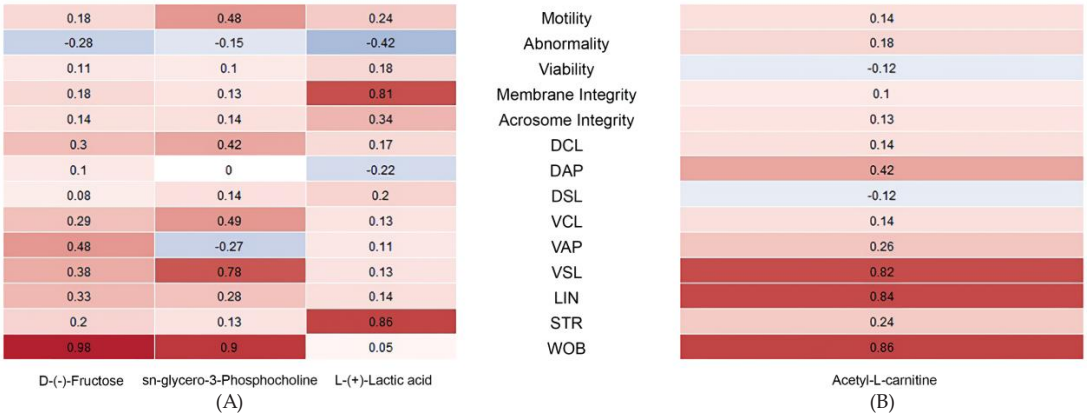

Figure 8. Correlation heatmap matrix revealing relationships among metabolite levels, sperm quality traits, and kinematic parameters in X- (A) and Y-bearing (B) spermatozoa of Holstein Friesian bulls. Red and blue colors indicate positive and negative correlations, respectively.

0.82), LIN (r = 0.84), and WOB (r = 0.86)—and revealing moderate correlations by DAP (r = 0.42) and VAP/STR (r ≈ 0.26/0.24). Correlations by total movement, live sperm, and membrane or acrosome health were weak (|r| ≤ ~0.18), and DSL had a small negative correlation (r ≈ −0.12). Overall, these outcomes suggest that in X sperm, carbohydrate and phosphocholine are linked to stable and straight movement, and lactic acid helps keep the membrane healthy. In Y sperm, acetyl-L-carnitine is more linked to fast, straight movement than overall sperm health.

DISCUSSION

This study aimed to find small-molecule markers that can tell the difference between X and Y sperm and connect them to semen quality and movement in humid tropical conditions. This helps address the problem of unstable field outcomes by sex-sorted semen. The outcomes in Table 1 reveal that X sperm had better overall movement and acrosome health, while Y sperm had stronger membranes, fewer shape problems, greater speeds (VCL, VAP, VSL), longer movement paths (DCL, DAP, DSL), and better straightness (STR). These differences suggest that X and Y sperm may use different energy strategies, not just small variations of the same system.

The metabolomic data support this biological interpretation. Both unsupervised and supervised multivariate analyses clearly separated X- and Y-bearing sperm, by tight inside-of-group dispersion (Figures 1–2), and hierarchical clustering grouped samples primarily by chromosomal type (Figure 4), indicating a coherent biochemical organization rather than random processing noise. Consistent univariate differences across features (Figure 3 and Table 3), along with a greater number of retained HMDB-annotated metabolites and greater mean peak intensities in X-sperm (Table 2), suggest that the phenotypic differences observed in Table 1 are underpinned by a definable molecular basis that is reproducible across specimens.

Inside this framework, X-bearing sperm appear to employ a carbohydrate-focused strategy. Enrichment of pathways related to glycolysis/gluconeogenesis, pyruvate metabolism, and other carbohydrate modules (Figure 6 and Table 4) aligns with elevated levels of D-(−)-fructose, L-(+)-lactic acid, and sn-glycerol-3-

phosphocholine (sn-GPC) among the top discriminatory metabolites (Figure 7). These metabolites also have positive links with stable movement and membrane health (Figure 8). Simply put, ATP made through glycolysis in the tail helps keep the flagellum beating. Lactate release through transporters helps control pH inside the cell and keep ion balance. These conditions help keep the sperm moving straight and protect the membrane after sorting and storage, matching the X sperm outcomes in Table 1 (Amaral, 2022; Lasorsa *et al*., 2023; Rotimi *et al*., 2024). The link between sn-glycerol-3-phosphocholine (sn-GPC) and stable movement suggests phosphocholine may help keep the membrane flexible and support signals needed for capacitation. This fits with earlier studies on lipids related to fertility in bull semen (Longobardi *et al*., 2020; Talluri *et al*., 2022). Among the pathways in Table 4, glycerophospholipid metabolism showed the biggest impact. This highlights the crucial role of membrane structures in controlling sperm movement and capacitation signals. This matches the sn-glycerol-3-phosphocholine (sn-GPC) patterns and their link to movement (Longobardi *et al*., 2020; Talluri *et al*., 2022; Correnti *et al*., 2023). For carbohydrate metabolism, the pathways of fructose, mannose, glycolysis, and pyruvate have a stronger effect on sperm function than other sugar pathways. This reveals that ATP made through glycolysis is very crucial to keep the sperm tail moving and to control lactate and pH levels. This matches the greater levels of D-(−)-fructose and L-(+)-lactate, which are linked to how the sperm moves (Amaral, 2022; Lasorsa *et al*., 2023; Rotimi *et al*., 2024). Overall, these patterns reveal that the types of membrane lipids and the glycolysis process are very crucial. They are key in connecting metabolite changes to how the sperm moves.

In contrast, Y-bearing sperm displayed a metabolic pattern linked to carnitine and oxidation. This fits with their faster and straighter movement. Acetyl-L-carnitine was a crucial metabolite (Figure 7) and was strongly related to movement speed (Figure 8). This happens because acetyl-L-carnitine helps bring acyl groups into the mitochondria, making energy production in the sperm midpiece more efficient. Changes in ether-lipid and glycerophospholipid metabolism (Figure 6; Table 4) reveal that the membrane lipids are being reorganized in a coordinated way. This may help the mitochondria work better and improve flagellar signaling. This process helps explain why Y-sperm have greater STR and speed values, as revealed in Table 1. These outcomes also indicate that Y-sperm depend more on oxidative metabolism, while X-sperm rely more on glycolysis. This pattern has also been seen in studies of bull sperm and seminal plasma. In astheno-oligozoospermic bulls, disrupted fatty acid and ketone body metabolism has been linked to reduced motility. Similarly, Correnti *et al.* (2023) reported that variations in acylcarnitines and phospholipids in seminal plasma were positively associated with sperm motility and morphology, reinforcing that metabolomic signatures are closely connected to fertility-related functional traits.

These mechanistic insights guide the selection of a minimal, translational biomarker panel. While ten features achieved perfect AUCs in internal cross-validation (Table 5), several did so through quasi-separation by extreme $\log_2$ fold-change values, a pattern that can lead to overestimating discriminative performance. Focusing on metabolites by well-defined, non-overlapping distributions—D-(−)-fructose, L-(+)-lactic acid, and sn-glycerol-3-phosphocholine (enriched in X-sperm) and acetyl-L-carnitine (enriched in Y-sperm)—recapitulates the class separation observed in Figures 1–2 while maintaining physiological relevance (Figure 7). Because each metabolite can be quantified via targeted LC–MS or enzymatic assays, this panel offers a practical tool for laboratory quality control, enabling verification of fraction identity and detection of atypical batches prior to field deployment, directly linking molecular signatures to the divergent motility phenotypes summarized in Table 1.

These outcomes can be directly used to improve extender formulas and help make better decisions on farms. The data in Figure 8, Figure 6, and Table 4 support making X-sperm media that give the right amount of glycolysis sources (like fructose) and choline/phosphocholine. This can help keep the sperm membrane strong and make their movement more stable, which matches the better motility and acrosome integrity seen in X-sperm (Table 1). On the other hand, the Y-sperm metabolite pattern in Figure 8 reveals that adding carnitine may help keep their movement straight and fast. Antioxidants can also help reduce oxidative stress, which could lower the STR and speed seen in Table 1. In humid tropical dairy systems like those in Indonesia, farmers still face problems such as heat stress, changing energy in feed, and weak cold storage, as mentioned in the Introduction. Utilizing the four-metabolite pattern (Figure 7) to help sort sperm batches and choose the right extender can be a helpful way to connect lab sperm separation with better pregnancy outcomes on farms (Mateus *et al*., 2023; Schmidt *et al*., 2024).

The strength of this study comes from several pieces of clear evidence: multivariate separation (Figures 1–2), steady univariate differences (Figure 3 and Table 3), clear sample grouping (Figure 4), logical pathway patterns (Figure 6 and Table 4), and strong links to phenotypes (Figure 8). All of these support a solid understanding of the different movement and quality patterns revealed in Table 1. Nonetheless, several crucial limitations should be considered when interpreting these outcomes. The sample size was modest, which may exaggerate apparent group separation even by cross-validation. Some AUC-perfect features in Table 5 reflect presence/absence patterns rather than stable quantitative changes. HMDB-based identifications in Table 3 may include isobaric or isomeric ambiguities, and many pathway hits rely on single-metabolite mappings, making enrichment outcomes hypothesis-generating rather than definitive. Potential confounding factors by sorting procedures, extender composition, and cryo-handling cannot be fully excluded, and the correlations revealed in Figure 8 do not establish causality or guarantee generalizability across bulls, seasons, or facilities.

Translating these outcomes into practical applications will require targeted quantification of the four-metabolite panel in independent cohorts, mechanistic manipulation of glycolytic substrates, choline donors, monocarboxylate transport, and carnitine in controlled media, and prospective evaluation of the metabolite score (Figure 7) in relation to conception or pregnancy outcomes under varying thermal and management conditions. Such studies would link the biochemical patterns in Tables 1–5 and Figures 1–8 to on-farm fertility outcomes, transforming a laboratory-based signature into a robust decision-making tool.

Overall, the combined analysis of movement and metabolite data reveals that X- and Y-sperm have different movement patterns. These differences are caused by how they use energy and how their membranes are built. X-sperm mainly use carbohydrate and phosphocholine pathways, which help keep the membrane stable and control how the sperm moves. In contrast, Y-sperm rely on a carnitine-based oxidative pathway that supports faster and straighter movement. These metabolic processes help explain the differences in sperm quality and movement patterns in Table 1. This study combines past models of sperm energy use with sex-sorted sperm performance, giving a practical view for dairy farms in humid tropical areas. However, the research only used frozen semen from one cattle breed and did not test fertility in live animals, different environments, or various insemination conditions. This means the outcomes still need more testing to prove their reliability and usefulness in real situations.

CONCLUSION

This study reveals that X- and Y-sperm have clear and consistent differences in both traits and metabolites. X-sperm have greater overall movement and better acrosome integrity. Y-sperm have stronger membrane integrity, fewer shape problems, and move faster in a straight line. The metabolomic analysis revealed clear biomarker differences. X-sperm had greater levels of D-(−)-fructose, L-(+)-lactic acid, and sn-glycerol-3-phosphocholine. Y-sperm had greater levels of acetyl-L-carnitine. These outcomes confirm that certain metabolites are linked to the differences in quality and movement among X- and Y-sperm.

CONFLICT OF INTEREST

The authors declare that there are no conflicts of interest, financial or personal, that could have influenced the work reported in this manuscript.

ACKNOWLEDGEMENT

This research was supported by the Regular Fundamental Research Funding by the Research and Community Service Program, Directorate of Research and Community Service, Ministry of Higher Education, Science, and Technology of the Republic of Indonesia (Grant Number: 069/C3/DT.05.00/PL/2025). The authors sincerely thank the Institute for Research and Community Service and the team at the Laboratory of Animal Reproduction, Faculty of Animal Science, Hasanuddin University, for their invaluable support.

DECLARATION OF GENERATIVE AI AND AI-ASSISTED TECHNOLOGIES IN THE WRITING PROCESS

During the writing process, none of the authors used generative AI or AI-assisted technologies.

REFERENCES

Álvarez Gallardo, H., Urbán Duarte, D., Velázquez Roque, A., & De La Torre Sánchez, J. F. (2024). Uso y evolución del sexado espermático en bovinos. Revisión. Revista Mexicana de Ciencias Pecuarias, 15(3), 641-668. https://doi.org/10.22319/rmcp.v15i3.6372

Amaral, A. (2022). Energy metabolism in mammalian sperm motility. WIREs Mechanisms of Disease, 14(5), e1569. https://doi.org/10.1002/wsbm.1569

Baharun, A., Iskandar, H., Maulana, T., Rahmi, A., Handarini, R., Pramartaa, I. Q., Pamungkas, F. A., Samsudewa, D., Kaiin, E. M., Agung, P. P., Gunawan, M., Duma, Y., Arifiantini, R. I., & Said, S. (2025). Sperm protein profiles and their correlation by DNA integrity and protamine deficiency in Donggala bulls (*Bos indicus*): Implications for fertility assessment. Veterinary World, 18(8), 2357. https://doi.org/10.14202/vetworld.2025.2357-2366

Capela, L., Leites, I., Romão, R., Lopes-da-Costa, L., & Pereira, R. M. L. N. (2022). Impact of heat stress on bovine sperm quality and competence. Animals, 12(8), 975. https://doi.org/10.3390/ani12080975

Cheng, Y., Grigorieff, N., Penczek, P. A., & Walz, T. (2015). A primer to single-particle cryo-electron microscopy. Cell, 161(3), 438-449. https://doi.org/10.1016/j.cell.2015.03.050

Correnti, S., Preianò, M., Fregola, A., Gamboni, F., Stephenson, D., Savino, R., D'Alessandro, A., & Terracciano, R. (2023). Seminal plasma untargeted metabolomic and lipidomic profiling for the identification of a novel panel of biomarkers and therapeutic targets related to male infertility. Frontiers in Pharmacology, 14, 1275832. https://doi.org/10.3389/fphar.2023.1275832

Dasgupta, M., Kumaresan, A., Saraf, K. K., Nag, P., Sinha, M. K., Aslam M. K. M., Karthikkeyan, G., Prasad, T. S. K., Modi, P. K., Datta, T. K., Ramesha, K., Manimaran, A., & Jeyakumar, S. (2022). Deep metabolomic profiling reveals alterations in fatty acid synthesis and ketone body degradations in spermatozoa and seminal plasma of astheno-oligozoospermic bulls. Frontiers in Veterinary Science, 8, 755560. https://doi.org/10.3389/fvets.2021.755560

Diansyah, A., Santos, S., Herdis, H., Yusuf, M., Toleng, A. L., Dagong, M. I. A., Priyatno, T. P., Maulana, T., Said, S., Iskandar, H., Nurlatifah, A., Lestari, P., Affandy, L., Baharun, A., & Rahmat, R. (2024). Identification of reproductive performance utilizing CASA and plasma seminal proteomics on Bali-Polled bull fertility. https://doi.org/10.22541/au.172506223.34281631/v1

Fadilla, Z. J., Yusuf, M., Toleng, A. L., & Diansyah, A. M. 2023. Characteristics and kinematics of Bali bull sperms after thawing utilizing tris soy lecithin. Journal of Advanced Zoology, 44(4), 477–487. https://doi.org/10.17762/jaz.v44i4.1967

Firdaus, A., Utami, P., Ramadhani, A., Syah, H. A., ShikhMaidin, M., Yekti, A. P. A., Isnaini, N., & Susilawati, T. (2024). Conception rate of filial Friesian Holstein cows after being inseminated utilizing unsexed and sexed semen.

Jurnal Ilmu-Ilmu Peternakan, 34(1), 99-107. https://doi.org/10.21776/ub.jiip.2024.034.01.11

Giaretta, E., Damato, A., Zennaro, L., Bonfatti, V., Mislei, B., Vigolo, V., Falomo, M. E., Bertuzzo, F., Gabai, G., & Bucci, D. (2025). Metabolome and oxidative stress markers in the seminal plasma of Holstein bulls and their relationship by the characteristics of fresh and frozen/thawed sperm. Theriogenology, 235, 262-274. https://doi.org/10.1016/j.theriogenology.2025.01.015

Hasan, I., Amalia, R., Yekti, A. P. A., Wahjuningsih, S., & Susilawati, T. (2023). Conception rate of artificial insemination utilizing sexed frozen semen by albumin sedimentation method on Friesian Holstein cow. BIO Web of Conferences, 81, 00016. https://doi.org/10.1051/bioconf/20238100016

Khan, I., Mesalam, A., Heo, Y. S., Lee, S. H., Nabi, G., & Kong, I. K. (2023). Heat stress as a barrier to successful reproduction and potential alleviation strategies in cattle. Animals, 13(14), 2359. https://doi.org/10.3390/ani13142359

Lasorsa, F., Di Meo, N. A., Rutigliano, M., Ferro, M., Terracciano, D., Tataru, O. S., Battaglia, M., Ditonno, P., & Lucarelli, G. (2023). Emerging hallmarks of metabolic reprogramming in prostate cancer. International Journal of Molecular Sciences, 24(2), 910. https://doi.org/10.3390/ijms24020910

Longobardi, V., Kosior, M. A., Pagano, N., Fatone, G., Staropoli, A., Vassetti, A., Vinale, F., Campanile, G., & Gasparrini, B. (2020). Changes in bull semen metabolome in relation to cryopreservation and fertility. Animals, 10(6), 1065. https://doi.org/10.3390/ani10061065

Mateus, F. G., Moreira, S., Martins, A. D., Oliveira, P. F., Alves, M. G., & Pereira, M. D. L. (2023). L-carnitine and male fertility: is supplementation beneficial?. Journal of Clinical Medicine, 12(18), 5796. https://doi.org/10.3390/jcm12185796

Nirmala, A., Toleng, A. L., Yusuf, M., Herdis, H., Diansyah, A. M., Amrullah, M. F., Rahmat, R., Rajamuddin, R., Alfian, A. M., & Hasrin, H. (2025). Effect of adding kasumba turate (*Carthamus tinctorius* L.) extract in tris-egg yolk diluent on sperm quality in Bali bulls. Journal of Animal Health and Production, 13(1), 154-159.. https://doi.org/10.17582/journal.jahp/2025/13.1.154.159

Nurcholis, N., Sumaryanti, L., Irianto, A., & Salamony, S. M. (2024). Fertilization rate of crossbreeding cattle utilizing sexing and conventional semen in different seasons in South Papua. Journal of Advanced Veterinary and Animal Research, 11(4), 954. https://doi.org/10.5455/javar.2024.k845

Ricci, L., Stanley, F. U., Eberhart, T., Mainini, F., Sumpton, D., & Cardaci, S. (2023). Pyruvate transamination and NAD biosynthesis enable proliferation of succinate dehydrogenase-deficient cells by supporting aerobic glycolysis. Cell Death & Disease, 14(7), 403. https://doi.org/10.1038/s41419-023-05927-5

Rotimi, D. E., Iyobhebhe, M., Oluwayemi, E. T., Olajide, O. P., Akinsanola, B. A., Evbuomwan, I. O., Asaleye, R. M., & Ojo, O. A. (2024). Energy metabolism and spermatogenesis. Heliyon, 10(19). https://doi.org/10.1016/j.heliyon.2024.e38591

Said, S., Arman, C., & Tappa, B. (2014). Conception rates and sex concomitant of Bali calves following oestrus synchronization and artificial insemination of frozen-sexed semen under farm conditions. Journal of the Indonesian Tropical Animal Agriculture, 39(1), 10-16. https://doi.org/10.14710/jitaa.39.1.10-16

Santoso, S., Herdis, H., Arifiantini, R. I., Gunawan, A., & Sumantri, C. (2021). Characteristics and potential production of frozen semen of Pasundan bull. Tropical Animal Science Journal, 44(1), 24-31. https://doi.org/10.5398/tasj.2021.44.1.24

Schmidt, C. A., Hale, B. J., Bhowmick, D., Miller, W. J., Neufer, P. D., & Geyer, C. B. (2024). Pyruvate modulation of redox potential controls mouse sperm motility. Developmental Cell, 59(1), 79-90. https://doi.org/10.1016/j.devcel.2023.11.011

Silva, W. C. D., Silva, J. A. R. D., Camargo-Júnior, R. N. C., Silva, É. B. R. D., Santos, M. R. P. D., Viana, R. B., Silva, A. G. M. e, Silva, C. M. G. da, & Lourenço-Júnior, J. D. B. (2023). Animal welfare and effects of per-female stress on male and cattle reproduction—A review. Frontiers in Veterinary Science, 10, 1083469. https://doi.org/10.3389/fvets.2023.1083469

Talluri, T. R., Kumaresan, A., Sinha, M. K., Paul, N., Ebenezer Samuel King, J. P., & Datta, T. K. (2022). Integrated multi-omics analyses reveals molecules governing sperm metabolism potentially influence bull fertility. Scientific Reports, 12(1), 10692. https://doi.org/10.1038/s41598-022-14589-w

Thongkham, M., Thaworn, W., Pattanawong, W., Teepatimakorn, S., Mekchay, S., & Sringarm, K. (2021). Spermatological parameters of immunologically sexed bull semen assessed by imaging flow cytometry, and dairy farm trial. Reproductive Biology, 21(2), 100486. https://doi.org/10.1016/j.repbio.2021.100486